Vol. 55: 135–151, 2012
doi: 10.3354/cr01124

CLIMATE RESEARCH
Clim Res

Published online December 13

Associating Michigan climate with low-level airflow trajectories and atmospheric teleconnections

Ryan P. Shadbolt[1,*]

[1]Department of Geography, Central Michigan University, Mount Pleasant, Michigan 48859, USA

ABSTRACT: The climate of Michigan is influenced by airflow circulation associated with atmospheric teleconnections. Previous studies have investigated mid-level airflow and atmospheric teleconnections, while low-level airflow has had less attention. Analyses of low-level airflow trajectories and atmospheric teleconnection associations are presented for a location in Lower Michigan. Airflow trajectories, which provide an important approach to monitoring changes in atmospheric circulation, are used to represent the low-level circulation during 1950–2011. A 5-day back-trajectory climatology for the 925 hPa pressure level was developed using the National Centers for Environmental Prediction (NCEP) and the National Center for Atmospheric Research (NCAR) reanalysis data archive. Low-level and mid-level circulation associated with the North Atlantic Oscillation (NAO), the Pacific/North American pattern (PNA), and El Niño/La Niña (NINO3.4) highlighted advection of heat and moisture during particular times of the year and the presence of single or simultaneous strong atmospheric teleconnections. The results indicate that airflow associated with teleconnections often differs seasonally. Additionally, trajectory patterns vary, based on whether a single strong teleconnection is present or if 2 strong teleconnections are coexisting. Using low-level airflow anomalies assists in bridging the gap between local-scale climate anomalies, such as temperature and precipitation, and atmospheric teleconnections. While a climatological study is presented here, the knowledge obtained could be applied in modeling and contribute to improved medium- and long-range forecasts.

KEY WORDS: Teleconnections · Trajectories · NAO · PNA · El Niño · La Niña · Michigan

Resale or republication not permitted without written consent of the publisher

1. INTRODUCTION

Local and regional temperature and precipitation anomalies have previously been related to atmospheric teleconnections (e.g. Yarnal & Leathers 1988, Leathers et al. 1991, Assel 1992, Serreze et al. 1998). However, fully bridging the gap between atmospheric teleconnections and local-scale climate anomalies is a task also requiring knowledge of the corresponding synoptic- and meso-scale phenomena. With this task in mind, the following study considered low-level trajectories in an effort to link together the relationships between atmospheric teleconnections and local-scale climate anomalies.

Many teleconnection studies focused attention on the southeastern USA (e.g. Ropelewski & Halpert 1986, 1987, 1989, Rohli & Rogers 1993, Henderson & Robinson 1994, Yin 1994, Mote 1996, Konrad 1998, Hardy & Henderson 2003), and the eastern USA (e.g. Wallace & Gutzler 1981, Wanner et al. 2001, Bradbury et al. 2002a,b). Generally, national studies have not found strong correlations between teleconnections and climate of Michigan or the Great Lakes region, which has led to a recent deficiency in teleconnection research for that region. Thus, a detailed regional study of teleconnections and the potential impact on Michigan's climate will likely be beneficial to future climate research not only of Michigan, but of the entire Great Lakes region as well.

*Email: shadb1rp@cmich.edu

© Inter-Research 2012 · www.int-res.com

Atmospheric teleconnection indices considered were the North Atlantic Oscillation (NAO), the Pacific/North American (PNA) pattern, and El Niño/La Niña (NINO3.4). These teleconnections were selected based on possible seasonal linkages with temperature and precipitation suggested in previous studies. While it is likely that other teleconnections affect Michigan on seasonal, annual, and decadal time scales, the results presented here focus on seasonal associations. These 3 frequently documented teleconnections were chosen in an effort to keep the potential number of teleconnection combinations manageable.

During eastern USA winters a strong positive phase of the NAO (NAO+) is associated with stronger westerlies and warmer temperatures, and conversely, a negative phase (NAO–) is associated with weaker westerlies and cooler temperatures (Wallace & Gutzler 1981, Rogers 1984, Yarnal & Leathers 1988, Assel & Rodionov 1998, Thompson & Wallace 2001, Wanner et al. 2001). Assel & Rodionov (1998) and Assel et al. (2004) also found the NAO to be negatively correlated with ice cover over the Great Lakes.

Wallace & Gutzler (1981) described how a positive phase of the PNA (PNA+) is associated with a pronounced ridge/trough pattern over North America and cooler temperatures over the eastern USA. In addition, Yarnal & Leathers (1988), Leathers et al. (1991), Assel (1992), Serreze et al. (1998), Coleman & Rogers (2003), and Rogers & Coleman (2004) showed that PNA+ is related with decreased precipitation in the Great Lakes region. On the other hand, zonal flow and above-normal temperatures exist during a strong negative phase of the PNA (PNA–) (Assel 1992, Rogers & Coleman 2004). Rogers & Rohli (1991) and Rohli & Rogers (1993) showed an increase in anticyclones traversing the Great Lakes during the meridional flow associated with PNA+, while Rodionov (1994) and Angel & Isard (1998) found an increase in cyclone frequency. Despite more cyclones, Rodionov (1994) pointed out that the majority of cyclones are of Alberta (Canada) origin, and thus less moisture and precipitation are usually involved because of the continental polar air mass present over that region. In contrast, during the zonal or trough/ridge flow associated with PNA–, cyclones originate to the west/southwest of the Great Lakes and such systems result in increased precipitation amounts (Rodionov 1994). The above PNA studies tended to focus on cool season months.

Some disagreement exists in the current literature regarding the effect of El Niño and the Southern Oscillation (ENSO) on the climate of the Great Lakes region. The discrepancies may be due to the fact that climate anomalies often differ between weak or strong ENSO phases (e.g. Rodionov & Assel 2000, 2003, Eichler & Higgins 2006, Aguado & Burt 2012). Hu & Feng (2001a, 2001b) related increased summer rainfall in the central USA with El Niño during epochs spanning 1871–1917 and 1948–1978. Increased wintertime temperatures, as well as a decrease in the frequency of cold-air outbreaks for the Great Lakes, were shown to be associated with the presence of El Niño (Gershunov & Barnett 1998, Changnon et al. 2000, Rodionov & Assel 2000, 2003, D'Aleo & Grube 2002, Eichler & Higgins 2006). Eichler & Higgins (2006) also concluded that drier (wetter) conditions are present in the Great Lakes during El Niño (La Niña) winters, respectively. During the 1997–1998 El Niño event, Changnon et al. (2000) found warmer and drier winter conditions for the Midwest, as well as drier conditions during spring, and cooler and wetter conditions during summer and autumn. In contrast, Harrison & Larkin (2002) showed warm conditions during El Niño winters and autumns, as well as cool conditions during El Niño springs, in Lower Michigan spanning 1946–1995. Rodionov et al. (2001) demonstrated a correspondence between past El Niño events and decreased ice cover over the Great Lakes. D'Aleo & Grube (2002) claimed that Midwest summer temperatures are warmer during La Niña, while Harrison & Larkin (2002) showed that La Niña winters and springs in the Midwest are warmer than usual, while La Niña autumns are colder. In general, past research suggests that the effects of NAO, PNA, and ENSO tend to be greatest on cool season conditions for the eastern USA.

In addition to using trajectories to relate teleconnections to local climate, this study also aimed to fill a void in the current literature regarding the behavior of interacting (i.e. coexisting) teleconnections. Most studies have primarily considered teleconnections individually. The behavior of the NAO during a strong phase of the PNA and/or ENSO, for example, remains largely unexplored territory. So far, previous research has suggested that PNA+ is common during El Niño periods (e.g. Renwick & Wallace 1996, Rodionov & Assel 2000, Coleman & Rogers 2003). Yarnal & Leathers (1988) showed that while the combined action of the NAO and PNA is important to the overall climate of the USA, the 2 patterns are independent of each other on inter-annual time scales. Rogers (1984) considered associations between the NAO and ENSO and concluded that these 2 patterns are also independent of one another. He highlighted the downward trend in the NAO during the middle part of the last century. He also concluded that the coexistence of strong phases of the NAO and ENSO most likely occurred by

chance. When using NINO3 sea-surface temperatures, Huang et al. (1998) found a stronger temporal coherence with the NAO. More recently, the Arctic Oscillation has been considered along with the Pacific Decadal Oscillation (e.g. Budikova 2005) and with ENSO (e.g. Budikova 2008).

It is important to keep in mind that many teleconnections have been defined and consideration of them all would quickly create an unmanageable number of teleconnection combinations. Therefore, my study does not make a claim that all local climate anomalies in Michigan are entirely explained by the phases of the NAO, PNA, and El Niño/La Niña. The discussion presented is based solely on the information garnered during this investigation, which did not include all possible variables.

Specific research questions addressed in the following pages include: (1) Does low-level circulation, as depicted by airflow trajectories, differ from the mean circulation over Michigan during seasons of strong single or coexisting teleconnection patterns? (2) During months of anomalous circulation associated with teleconnections, can relationships be drawn between the trajectory patterns and local-scale climate? (3) Does the association of single or coexisting teleconnections with trajectories and local-scale climate vary by season?

2. DATA AND METHODS

2.1. Teleconnection indices

Monthly values of NAO and PNA indices were obtained from the Climate Prediction Center (CPC) (ftp.cpc.ncep.noaa.gov/wd52dg/data/indices/tele_index.nh) and were calculated using a multi-step approach based on earlier work by Barnston & Livezey (1987). Values were standardized to give monthly indices a mean of zero and a standard deviation of 1.0. El Niño/La Niña anomaly values were obtained from the CPC's NINO3.4 dataset (www.cpc.ncep.noaa.gov/data/indices/ersst3b.nino.mth.ascii).

For each month during the 1950–2011 study period, the NAO and PNA were defined as being in a strong positive phase (index value ≥1.0), a strong negative phase (index value ≤–1.0), or a neutral phase (<1.0 and >–1.0) in a similar manner to previous studies (e.g. Yin 1994, Vega et al. 1998, Englehart & Douglas 2003, Hardy & Henderson 2003, Sheridan 2003). For NINO3.4, a threshold of ≥0.5 was used to determine El Niño events and ≤–0.5 was used for La Niña events (e.g. Higgins et al. 2002). In most cases zero or 1 of the 3 teleconnections was in a strong phase. However, instances of 2 or more teleconnections simultaneously having a strong positive or negative phase did occur. Months were categorized as either 'single teleconnection' or 'coexisting teleconnection' events and then classified by which teleconnection index (indices) was (were) active. With 3 teleconnections and 3 possible phases for each (negative, neutral, or positive), a total of 27 teleconnection combinations were possible. Furthermore, months with the same teleconnection combination were grouped into the 4 meteorological seasons: winter (December to February), spring (March to May), summer (June to August), and autumn (September to November), resulting in 108 potential combinations. Of the 108 combinations, many occurred infrequently or not at all. To ensure a sufficient number of events for statistical analysis, only those seasonal teleconnection combinations with 10 or more occurrences were retained. A minimum cutoff of 10 occurrences meant that all teleconnection combinations presented here had a seasonal frequency of at least 5.0% over the 1950–2011 period.

2.2. Low-level airflow trajectories and mid-level height anomalies

Typical low-level seasonal airflow for the study area was compared to airflow during coexisting tele-

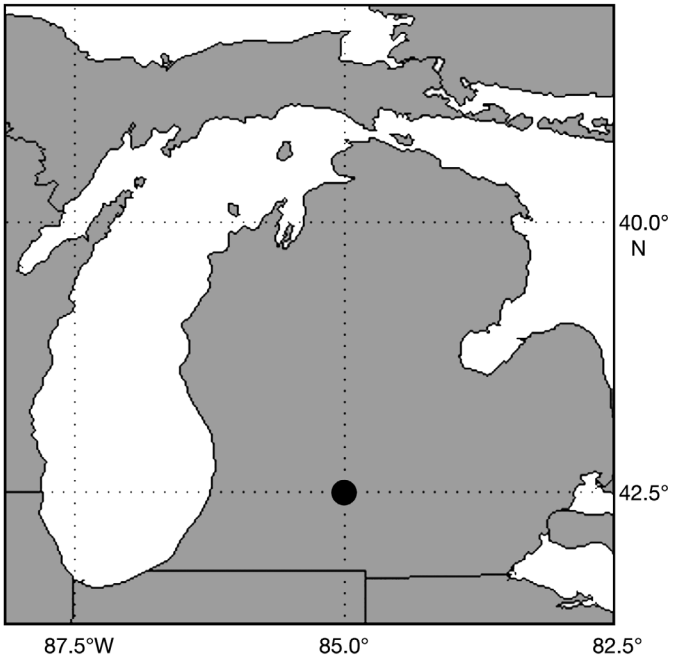

Fig. 1. Terminus point (●; 42.5° N, 85.0° W) for the airflow trajectories in Lower Michigan, USA

connections. Trajectories used here were calculated following a procedure developed by Shadbolt et al. (2006), where trajectories were used to identify air mass source regions for Lower Michigan. Michigan was chosen because it experiences large seasonal variations in temperature and precipitation associated with airflow from multiple source regions. Five-day back trajectories to a terminus point located over central Lower Michigan (Fig. 1) were used to represent airflow. The trajectories were calculated 4 times per day along the 925 hPa isobaric surface using wind fields from the National Centers for Environmental Prediction (NCEP) and the National Center for Atmospheric Research (NCAR) reanalysis (Kalnay et al. 1996, Kistler et al. 2001). The 925 hPa trajectory locations were calculated and archived in 3-h time steps, referred to as trajectory nodes, with each node having an associating latitude, longitude, and date.

For each seasonal teleconnection combination, trajectory nodes were assigned to 0.5° × 0.5° grid cells and the number of nodes within each cell was counted. Areas of greater node density represent low-level airflow 'corridors' that can be traced from the terminus point to air mass source regions. To facilitate comparison between the seasonal climatology and teleconnection combinations, grid cell densities for both the teleconnection combinations and for the seasonal climatologies were divided by the respective maximum possible number of nodes (i.e. the number of nodes summed across all grid cells). The resulting grid cell values for the teleconnection combinations were then subtracted from the respective seasonal climatology grid cell values to determine a deviation value. Anomalies were plotted by standard deviation, where positive values depict airflow corridors that have more trajectory nodes than the seasonal climatology, and negative values depict airflow corridors that have fewer trajectory nodes than the seasonal climatology.

Mid-level airflow was represented by 500 hPa height values. The dataset was also obtained from the NCEP/NCAR reanalysis. Climatologies of 500 hPa heights were created for each season. Height anomaly values were then calculated for each seasonal teleconnection combination. Considering low-level trajectories and mid-level height values provides a better depiction of both meso- and synoptic-scale flow associated with the teleconnections.

Table 1. Frequency (%) and number of monthly occurrences of seasonal teleconnection combinations (occurrences of 10 or more are in **bold**) during the period 1950–2011. North Atlantic Oscillation (NAO), Pacific/North American (PNA) pattern, and El Niño/La Niña (NINO). +/–: positive or negative phase of the teleconnection (see Section 2.1. for details on phases)

Teleconnection combination	Winter Freq. (%)	N	Spring Freq. (%)	N	Summer Freq. (%)	N	Autumn Freq. (%)	N
All neutral	**12.9**	**24**	**21.5**	**40**	**21.0**	**39**	**15.1**	**28**
NAO+	1.6	3	**6.5**	**12**	**7.5**	**14**	4.8	9
NAO–	3.8	7	**9.7**	**18**	**5.4**	**10**	3.8	7
PNA+	4.8	9	3.2	6	**5.4**	**10**	**5.9**	**11**
PNA–	**6.5**	**12**	**5.9**	**11**	4.3	8	3.8	7
NINO+	**10.2**	**19**	**9.1**	**17**	**10.2**	**19**	**10.2**	**19**
NINO–	**11.3**	**21**	**13.4**	**25**	**9.7**	**18**	**15.6**	**29**
NAO+, PNA+	0.0	0	0.5	1	1.1	2	1.1	2
NAO+, PNA–	1.1	2	1.1	2	2.7	5	0.5	1
NAO+, NINO+	2.7	5	1.1	2	3.8	7	4.3	8
NAO+, NINO–	1.6	3	1.6	3	2.7	5	**5.4**	**10**
NAO–, PNA+	1.6	3	1.1	2	2.2	4	0.5	1
NAO–, PNA–	4.3	8	2.2	4	3.2	6	0.0	0
NAO–, NINO+	**6.5**	**12**	2.7	5	2.7	5	**5.9**	**11**
NAO–, NINO–	4.3	8	3.2	6	2.7	5	3.2	6
PNA+, NINO+	2.2	4	3.8	7	1.6	3	3.2	6
PNA+, NINO–	1.1	2	0.5	1	2.7	5	4.3	8
PNA–, NINO+	0.5	1	0.5	1	2.7	5	2.7	5
PNA–, NINO–	**10.2**	**19**	**5.4**	**10**	3.8	7	1.6	3
NAO+, PNA+, NINO+	0.5	1	1.1	2	0.5	1	2.2	4
NAO+, PNA+, NINO–	0.5	1	0.0	0	0.5	1	1.1	2
NAO+, PNA–, NINO+	1.1	2	0.0	0	0.5	1	0.5	1
NAO+, PNA–, NINO–	1.1	2	2.2	4	1.1	2	1.6	3
NAO–, PNA+, NINO+	2.2	4	1.1	2	1.1	2	0.0	0
NAO–, PNA+, NINO–	1.6	3	0.5	1	0.5	1	0.5	1
NAO–, PNA–, NINO+	3.2	6	0.5	1	0.5	1	1.1	2
NAO–, PNA–, NINO–	2.7	5	1.6	3	0.0	0	1.1	2

2.3. Temperature and precipitation anomalies

To further interpret the associations of teleconnection combinations, trajectory patterns, and local climate, monthly temperature and precipitation data for the local climate division in which the terminus point is located (Fig. 1) were obtained from the Climate Diagnostics Center (CDC) (www.esrl.noaa.gov/psd/data/timeseries/). Monthly temperature and precipitation anomalies were calculated by subtracting the monthly means for the 1950–2011 period, and then the anomalies were averaged for each seasonal teleconnection combination. A *t*-test was used to determine whether or not the temperature and precipitation anomalies associated with each seasonal teleconnection combination were statistically different than zero at alpha (α) values of 0.01 and 0.05.

3. RESULTS AND DISCUSSION

3.1. Overview

Maps were produced for all seasonal teleconnection combinations that had at least 10 occurrences except for the seasonal combinations when all 3 teleconnections were in neutral phases. Table 1 highlights that the scenario of all 3 teleconnections having a neutral phase was the most common. Single teleconnection combinations (where 1 teleconnection is strong, but the other 2 are neutral) occurred with the second-most frequency. Coexisting teleconnection combinations with 2 strong and 1 neutral teleconnection occurred third most frequently. Lastly, coexisting teleconnection combinations where all 3 teleconnections were strong occurred with the least frequency. Temperature (Table 2) and precipitation (Table 3) anomalies are also provided for teleconnection combinations having a frequency of 5.0% or greater.

Table 2. Seasonal temperature (°C) anomalies during frequent seasonal teleconnection combinations. Statistically significant anomalies: $^{*}\alpha \leq 0.05$, $^{**}\alpha \leq 0.01$. Temperature anomalies are not provided for seasons of infrequent teleconnection combinations

Teleconnection combination	Temperature (°C)			
	Winter	Spring	Summer	Autumn
All neutral	0.7	0.3	−0.1	0.6
NAO+		1.7**	−0.2	
NAO−		−2.4**	0.4	
PNA+			−0.0	−2.0**
PNA−	0.5	−1.6*		
NINO+	1.2*	0.5	−0.0	−0.3
NINO−	−0.0	0.3	0.8**	0.7
NAO+, NINO−				1.0*
NAO−, NINO+	−1.1			−2.0**
PNA−, NINO−	0.6	−0.4		

Table 3. Seasonal precipitation (mm) anomalies during frequent seasonal teleconnection combinations. Statistically significant anomalies: $^{*}\alpha \leq 0.05$, $^{**}\alpha \leq 0.01$. Precipitation anomalies are not provided for seasons of infrequent teleconnection combinations

Teleconnection combination	Precipitation (mm)			
	Winter	Spring	Summer	Autumn
All neutral	−0.7	2.2	2.1	7.1
NAO+		−11.9	0.6	
NAO−		−8.0	−3.3	
PNA+			6.2	−24.7**
PNA−	3.7	17.0		
NINO+	4.7	−1.2	1.3	6.9
NINO−	9.1	−10.5	−4.7	−7.2
NAO+, NINO−				−4.1
NAO−, NINO+	−17.2**			−7.2
PNA−, NINO−	12.9*	13.5*		

Fig. 2 shows seasonal 925 hPa trajectory and 500 hPa height climatologies for Lower Michigan. During a typical winter season (Fig. 2a,b) the 925 hPa back-trajectory airflow consists of a broad northwesterly corridor and smaller westerly and southerly corridors. Spring (Fig. 2c,d) shows increased airflow from the north, particularly originating around Hudson Bay, as well as a southerly corridor that originates near the Gulf of Mexico. Summer (Fig. 2e,f) is associated with a distinct southerly corridor, smaller northwesterly and northerly corridors, and more trajectory nodes existing close to the terminus point. Lastly, autumn (Fig. 2g,h) shows a broad northwesterly corridor again and a southerly corridor that does not originate as far over the Gulf. The grid values from these seasonal 925 hPa trajectory and 500 hPa height climatologies were used to calculate the airflow anomaly values for the seasonal teleconnection combination results presented below. Trajectory analyses for neighboring grid points around the Great Lakes region spanning 40.0–45.0° N and 82.5–87.5° W were conducted and resulted in nearly identical results to those shown in Fig. 2, supporting that the trajectory results shown here for 42.5° N and 85.0° W are applicable to not just Lower Michigan, but for the surrounding Great Lakes region.

3.2. Neutral phases

Situations where all 3 teleconnections were in a neutral phase were by far the most common. Over the 1950–2011 period, the neutral combination occurred 12.9% of the time in winter, 21.5% of the time in spring, 21.0% of the time in summer, and 15.1% of the time in autumn (Table 1). These results indicate that the neutral combination occurred more frequently in the warm season than during the cool season. Statistically significant climate anomalies were not experienced with the neutral combination (maps not shown).

3.3. Single strong teleconnections

3.3.1. NAO

NAO+ was most frequent in spring (6.5%) and summer (7.5%). The spring trajectory pattern (Fig. 3a) shows fewer-than-average trajectories from

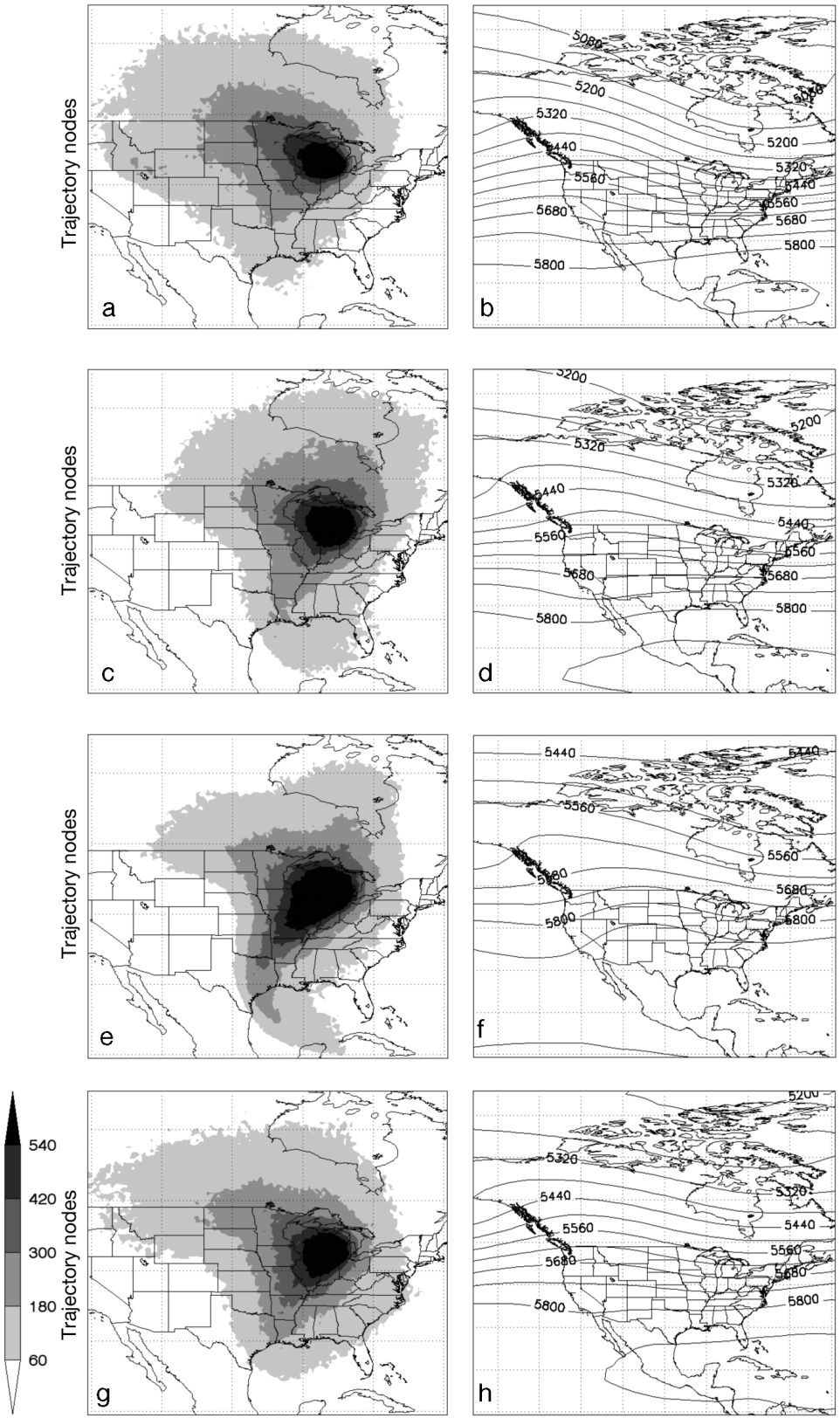

Fig. 2. Seasonal 925 hPa trajectory node (left) and 500 hPa height (m) climatologies (right) for Lower Michigan (1950–2011): (a,b) winter, (c,d) spring, (e,f) summer, (g,h) autumn

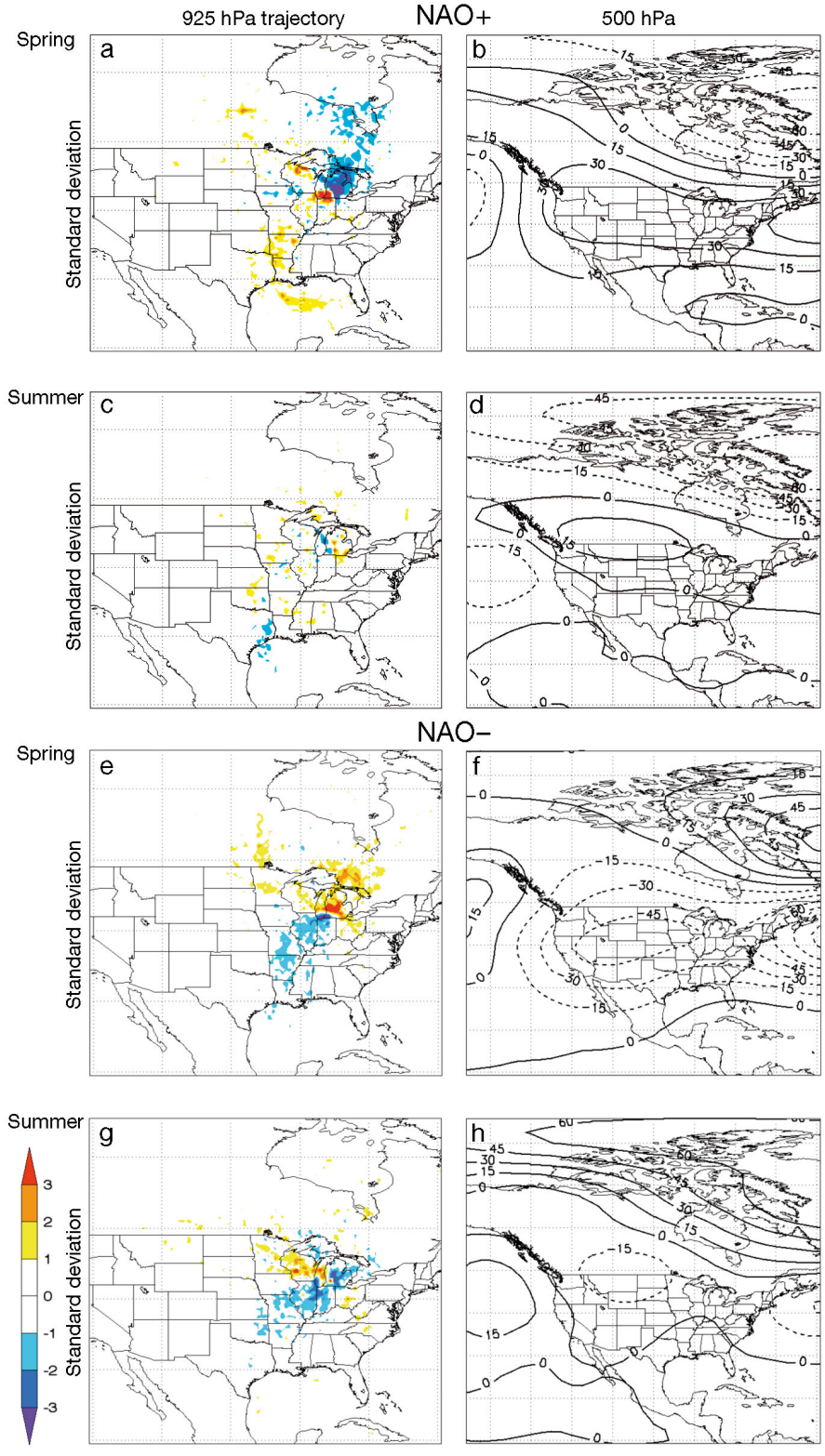

Fig. 3. Seasonal 925 hPa trajectory anomalies (left) and 500 hPa height (m) anomalies (right) under positive and negative North Atlantic Oscillation (NAO) phases: (a,b) NAO+ spring, (c,d) NAO+ summer, (e,f) NAO− spring, (g,h) NAO− summer. Red tones indicate areas of higher trajectory density and blue tones indicate areas of decreased trajectory density compared to the corresponding seasonal trajectory climatology in Fig. 2. Solid contours represent positive height anomalies, while dashed contours represent negative height anomalies

the north and increased flow from the south. The spring 500 hPa heights (Fig. 3b) are in agreement with past research, showing the increased pressure gradient between the Icelandic Low and the Bermuda High, and suggesting stronger southerly or westerly winds at mid-levels over Michigan. The presence of the strong Bermuda High appears to be the driving force for the increased flow originating over the Gulf of Mexico. Increased 500 hPa heights and the southerly low-level flow corresponded with warm-air advection and a significant warm temperature anomaly of 1.7°C (significant at $\alpha = 0.01$). However, the precipitation anomaly was insignificant. NAO+ during summer was also associated with some minor increases in southerly flow (Fig. 3c) and higher-than-normal height values (Fig. 3d), but did not exhibit significant climate anomalies.

NAO− also occurred frequently in spring (9.7%) and summer (5.4%). Maps for spring (Fig. 3e,f) show an increase in low-level trajectory frequency to the north of the terminus point and a decrease in trajectory frequency to the south along with lower-than-normal 500 hPa height values over the USA. The much weaker Bermuda High corresponded to a cool temperature anomaly for spring (−2.4°C; significant at $\alpha = 0.01$). Summer trajectories (Fig. 3g) also show decreased southerly flow, but the increase in northerly flow is much less obvious. The overall summer 500 hPa pressure gradient (Fig. 3h) was also much weaker compared to spring, and no significant climate anomalies resulted.

Past literature also supports associations of NAO+ with warmer-than-normal temperatures and increased frequency of southerly flow over the eastern USA with no strong relationship to precipitation, while NAO− is associated with increased frequency of northerly upper-level airflow and cooler-than-normal temperatures (Wallace & Gutzler 1981, Rogers 1984, Yarnal & Leathers 1988, Assel & Rodionov 1998, Thompson & Wallace 2001, Wanner et al. 2001). One difference is that most previous studies focused on the winter season months, whereas here the strongest NAO associations were actually most common during spring.

3.3.2. PNA

Previous studies have usually considered PNA during winter months. However, this study instead found strong phases of PNA+ to be common only during summer (5.4%) and autumn (5.9%). In the past PNA+ has been found to be weak or non-existent during summer months; however, some strong index values were found in this study. Summer low-level trajectories (Fig. 4a) highlight increased southerly flow leading into Michigan, although the summer 500 hPa height gradient (Fig. 4b) bears little resemblance to the traditional PNA+ pattern, suggesting that, despite the significant index values, PNA+ plays only a minor role in summer circulation. This point is further supported by the fact that no significant climate anomalies occurred during summer (Tables 2 & 3). In contrast, the autumn season shows the more typical PNA+ relationships of decreased southerly flow and increased northerly/northwesterly flow (Fig. 4c), with 500 hPa heights (Fig. 4d) more clearly depicting a strengthened ridge over the western USA and a trough over the eastern USA. The resulting cold temperature anomaly (−2.0°C) and dry precipitation anomaly (−24.7 mm) were both significant at the $\alpha = 0.01$ level, suggesting that the northerly/northwesterly flow and mid-level convergence downstream of the ridge were responsible for the cold and dry conditions at the surface. These autumn results agreed with previous studies reporting that the PNA+ corresponded to increased northerly/northwesterly flow, a decrease in southerly flow, and cool and dry conditions (Wallace & Gutzler 1981, Yarnal & Leathers 1988, Leathers et al. 1991, Rogers & Rohli 1991, Assel 1992, Rohli & Rogers 1993, Rodionov 1994, Serreze et al. 1998, Coleman & Rogers 2003, Rogers & Coleman 2004).

Unlike PNA+, a strong PNA− occurred most frequently in winter (6.5%) and spring (5.9%). Winter trajectories (Fig. 4e) show a decrease in northerly and northwesterly trajectory node frequencies, with increases of westerly and southwesterly flow. The winter 500 hPa height anomalies (Fig. 4f) also show lower values over Canada and higher values over the southeastern USA, suggesting the possibility of a trough/ridge presence over the USA and an explanation for the increase in southwesterly low-level flow. Despite these apparent winter circulation anomalies, the corresponding temperature and precipitation anomalies were not significant (Tables 2 & 3). However, during spring, some increased trajectory node frequencies were present to the north, west, and south of the terminus (Fig. 4g). Previous literature has described how PNA− is associated with more zonal or westerly/southwesterly airflow, which could contribute to warmer temperatures and increased precipitation (Wallace & Gutzler 1981, Yarnal & Leathers 1988, Leathers et al. 1991, Rogers & Rohli 1991, Assel 1992, Rohli & Rogers 1993, Rodionov 1994, Serreze et al. 1998, Coleman & Rogers 2003, Rogers & Coleman

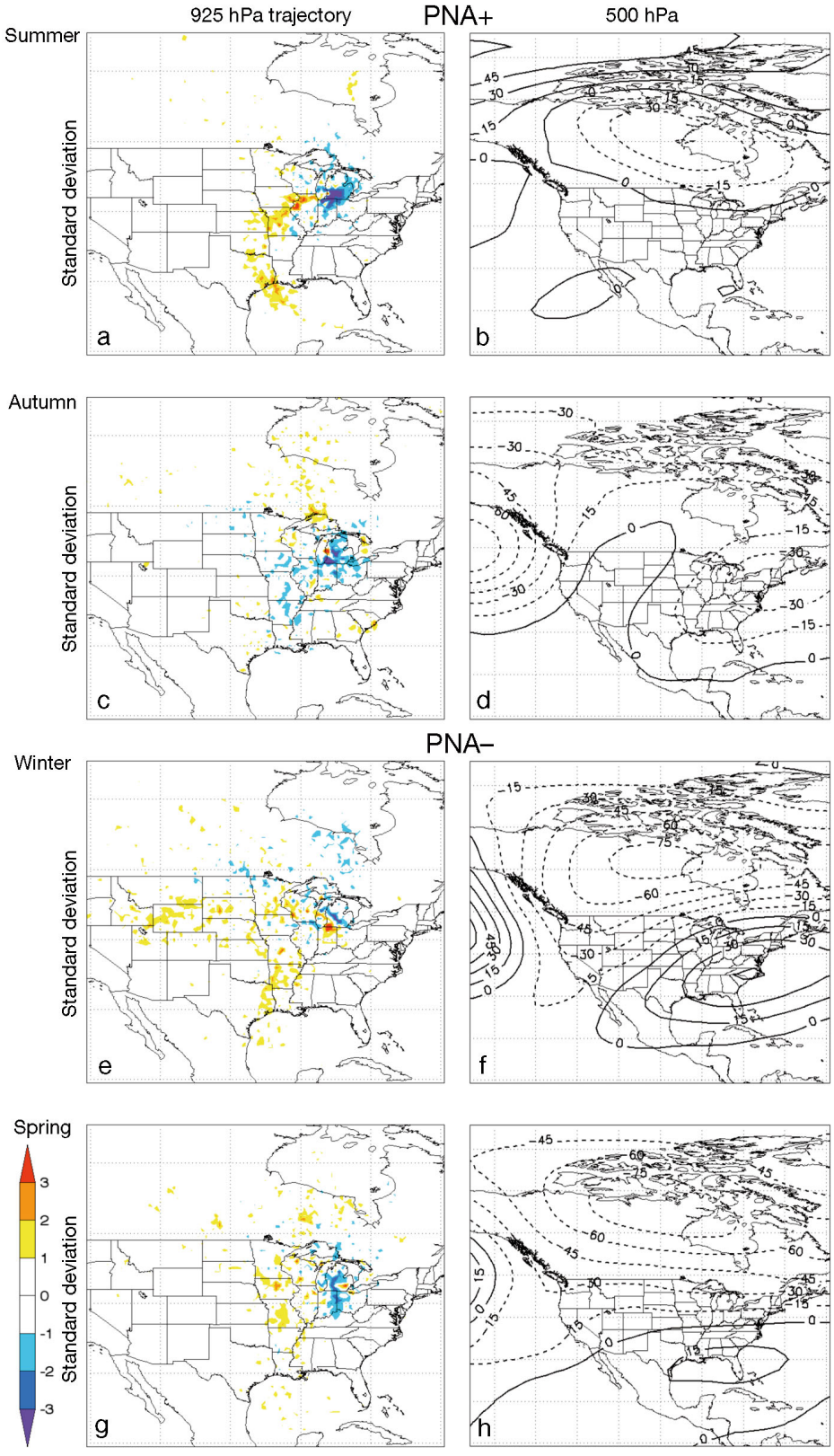

Fig. 4. Seasonal 925 hPa trajectory anomalies (left) and 500 hPa height (m) anomalies (right) under positive and negative Pacific/North American (PNA) pattern phases: (a,b) PNA+ summer, (c,d) PNA+ autumn, (e,f) PNA– winter, (g,h) PNA– spring. See Fig. 3 legend for explanation of colors and lines

2004). The spring 500 hPa height anomalies in the present study (Fig. 4h) are in agreement with these findings, showing a moderate pressure gradient suggesting zonal flow. Heights over Michigan during spring were lower than normal, however, and were reflected by the significant cool temperature anomaly of −1.6°C (significant at $\alpha = 0.05$). The springtime precipitation anomaly was insignificant (Table 3). The lower height values to the north appear to be responsible for the increased low-level flow from the north.

3.3.3. NINO3.4

NINO+ (El Niño) occurred frequently across all seasons: winter (10.2%), spring (9.1%), summer (10.2%), and autumn (10.2%). Trajectory anomalies for the NINO+ pattern differed throughout the year. Past authors have generally agreed that, over the Midwest, a strong El Niño is related to warmer temperatures and decreased precipitation in the winter season (Gershunov & Barnett 1998, Changnon et al. 2000, Rodionov & Assel 2000, 2003, D'Aleo & Grube 2002, Eichler & Higgins 2006). The winter trajectory map (Fig. 5a) does not exhibit strong patterns, but does illustrate fewer-than-normal trajectories originating to the northwest of the terminus. The winter 500 hPa heights (Fig. 5b) show a more distinct pattern of high values present over Canada. This pattern is consistent with previous research (Climate Prediction Center 2005, availabe at www.cpc.ncep.noaa.gov/products/analysis_monitoring/ensocycle/enso_cycle.shtml) that suggests a splitting of the polar jet, with a strong jet present over the southern USA and a second jet present over Canada. The ridging present over Michigan corresponded to a warm anomaly of 1.2°C (significant at $\alpha = 0.05$), although the precipitation anomaly was insignificant (Tables 2 & 3). With regard to other seasons, previous research has cited colder temperatures and decreased precipitation during spring (Changnon et al. 2000, Harrison & Larkin 2002), and cooler/wetter conditions during summer (Changnon et al. 2000). However, for autumn, Changnon et al. (2000) suggested that cooler/wetter conditions should be expected, while Harrison & Larkin (2002) reported that El Niño autumns are warm. In the present study, although a strong NINO+ existed, no significant climate anomalies were found for spring, summer, or autumn (Table 3). The low-level trajectory and mid-level height maps (Fig. 5c–h) show variation across the seasons, but generally the 3 seasons all show small 500 hPa height anomalies suggesting a weak pressure gradient and weak winds. Weak low-level winds are further supported by many positive trajectory anomalies near the terminus. These conditions led to temperature and precipitation values close to expected seasonal values.

NINO− (La Niña) also occurred during all seasons and was frequent 11.3% of the time during winters, 13.4% of springs, 9.7% of summers, and 15.6% of autumns. Previous literature suggests warmer and wetter conditions for Michigan during a La Niña winter or spring (Harrison & Larkin 2002, Eichler & Higgins 2006). In contrast, the present study did not find any significant climate anomalies in either season. A decrease in low-level flow from the northwest for winter is shown in Fig. 6a. La Niña has been shown to correspond to a strong ridge over the western USA and a trough over the eastern USA. The winter 500 hPa heights in Fig. 6b show a similar pattern, but the trough is very weak, which is probably the reason for the insignificant climate anomalies. Spring shows a decline in southerly trajectories (Fig. 6c) and weak height anomalies (Fig. 6d), with no significant climate anomalies (Tables 2 & 3). Previously, La Niña has been associated with warmer conditions during summer (D'Aleo & Grube 2002). The present study also found a significant warm anomaly evident in summer (0.8°C; significant at $\alpha = 0.01$). Summer low-level trajectories do suggest an increase in southerly flow (Fig. 6e), although it appears that the mid-level flow at 500 hPa (Fig. 6f) is not directly responsible for steering this since the 500 hPa height values tended to be close to typical seasonal flow. Low-level (Fig. 6g) and mid-level (Fig. 6h) flows for autumn were quite similar to summer La Niña conditions, but no significant climate anomalies were found (Tables 2 & 3). Harrison & Larkin (2002) reached the same conclusion for precipitation over the Midwest; however, they did describe cooler-than-normal conditions for autumn.

3.4. Simultaneous strong teleconnections

A coexisting NAO+ and NINO− occurred 5.4% of the time during autumn. NAO+ during autumn was not described above because it did not occur frequently. However, maps resulting from this combination (not shown) suggested stronger-than-normal westerly flow at low and mid levels. As described previously, Figs. 6g for La Niña showed an increase in southerly low-level flow. When considering NAO+ and NINO− together, there is also an increase in southerly low-level flow in autumn (Fig. 7a). How-

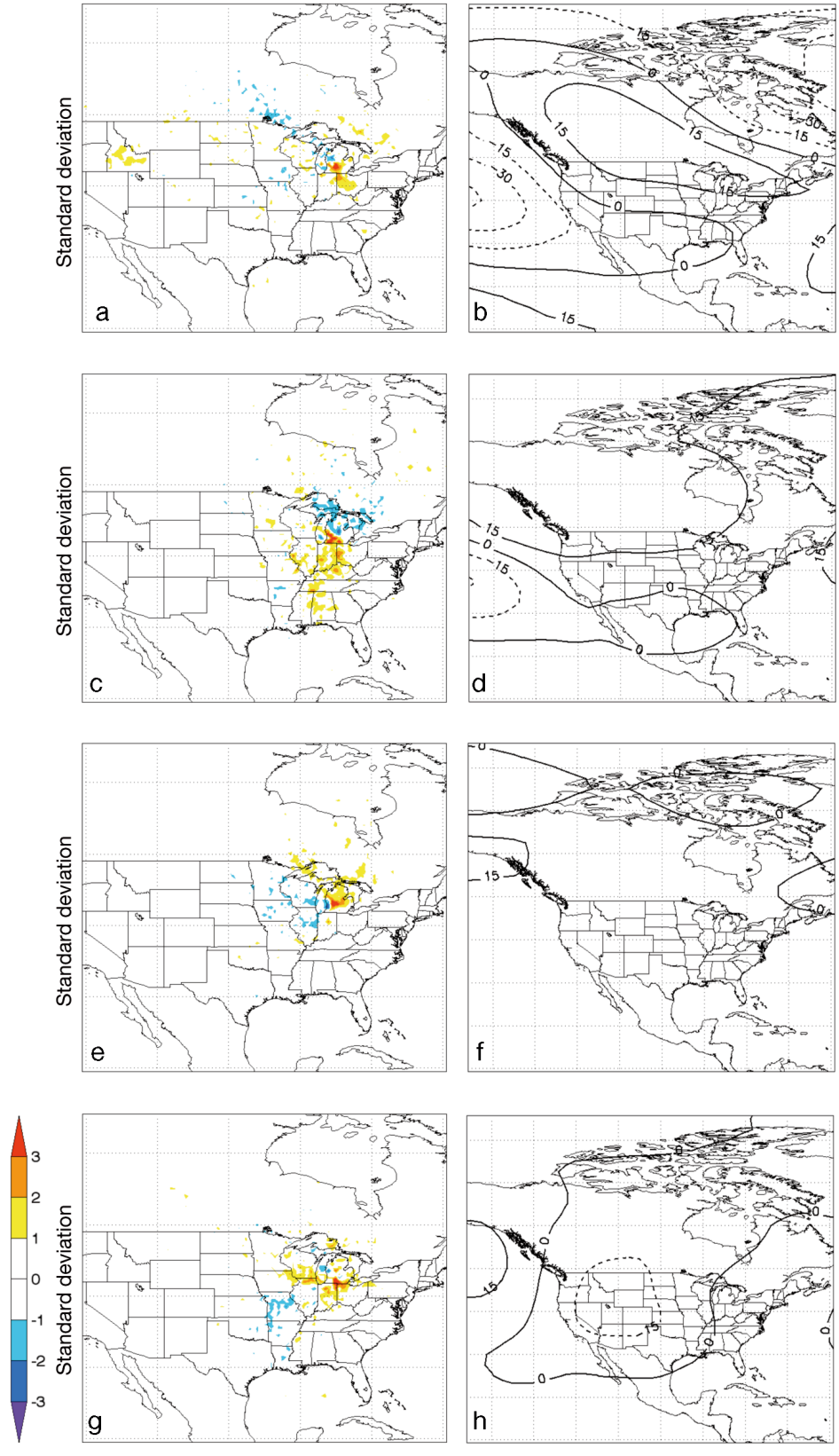

Fig. 5. El Niño (NINO+) seasonal 925 hPa trajectory anomalies (left) and 500 hPa height (m) anomalies (right): (a,b) winter, (c.d) spring, (e,f) summer, (g,h) autumn. See Fig. 3 legend for explanation of colors and lines

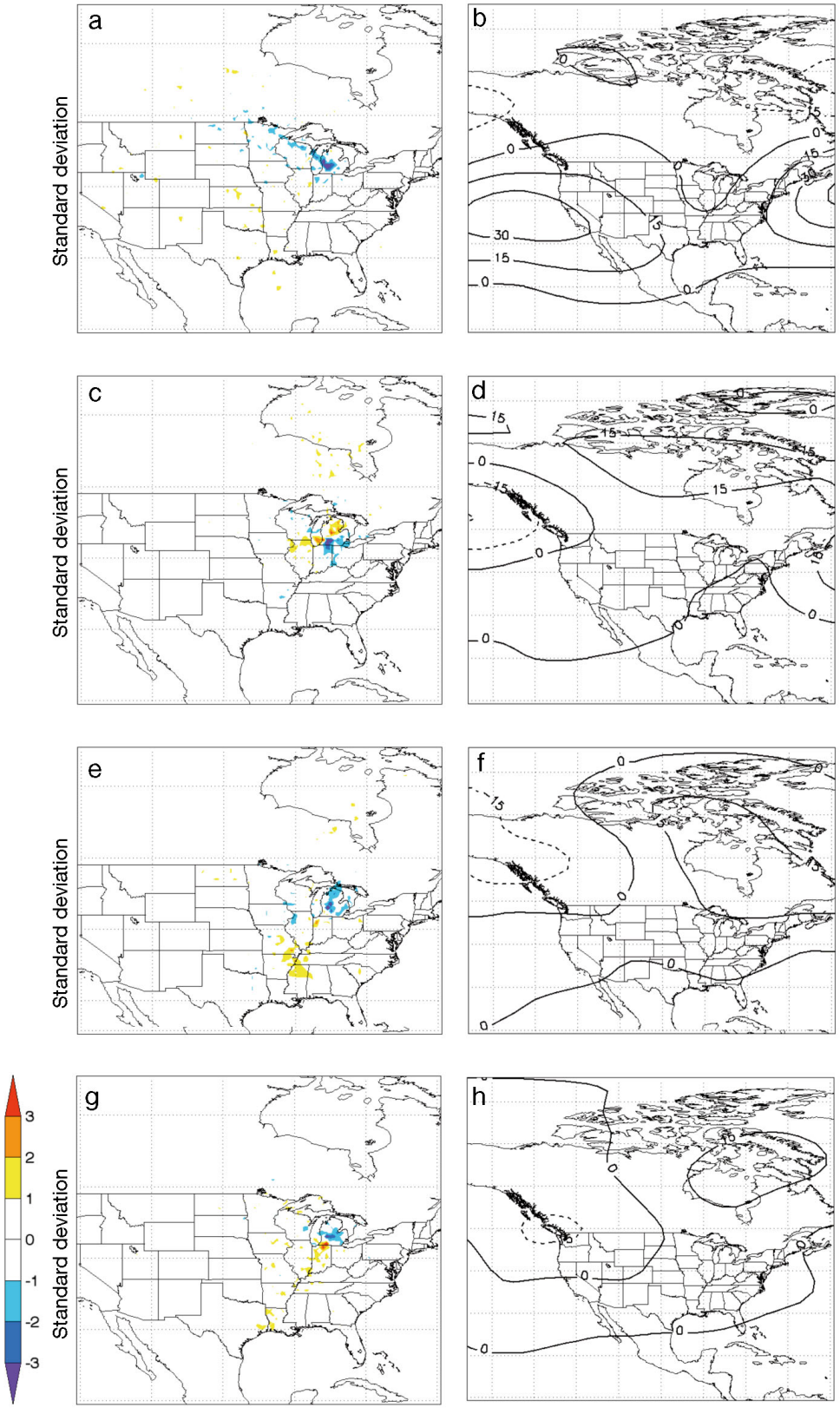

Fig. 6. La Niña (NINO–) seasonal 925 hPa trajectory anomalies (left) and 500 hPa height (m) anomalies (right): (a,b) winter, (c,d) spring, (e,f) summer, (g,h) autumn. See Fig. 3 legend for explanation of colors and lines

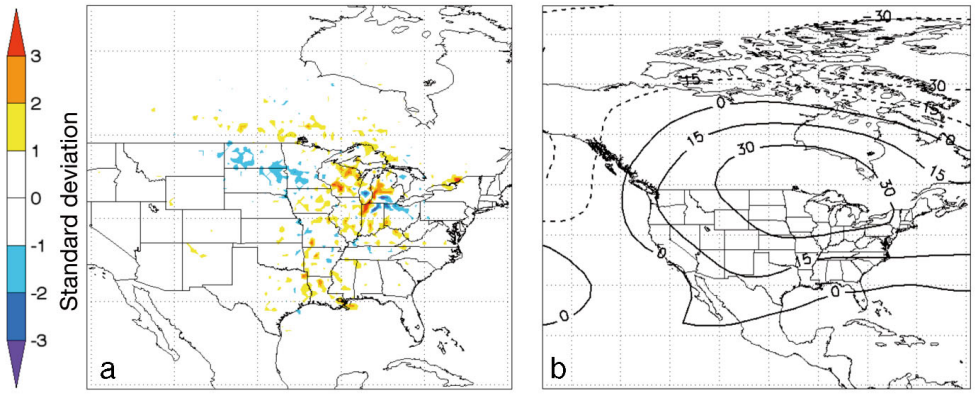

Fig. 7. Combined NAO+ and NINO− anomalies in autumn: (a) 925 hPa trajectory, (b) 500 hPa height (m). See Fig. 3 legend for explanation of colors and lines

ever, in contrast to Fig. 6h for NINO−, there is now a stronger pressure gradient present over the interior USA at 500 hPa (Fig. 7b). The ridge present over the study region corresponded to a significant temperature anomaly for autumn (1.0°C; significant at α = 0.05). The stronger pressure gradient shows some similarities to NAO+ flow, although the Icelandic Low is weaker and the highest anomalies tend to be over the continent rather than in the vicinity of the Bermuda High. The presence of the ridge may contribute toward steering the polar jet location to a more northward location than is typical for NAO+ conditions.

A simultaneous NAO− and NINO+ situation occurred during winter (6.5% frequency) and autumn (5.9% frequency). NAO− was described above for

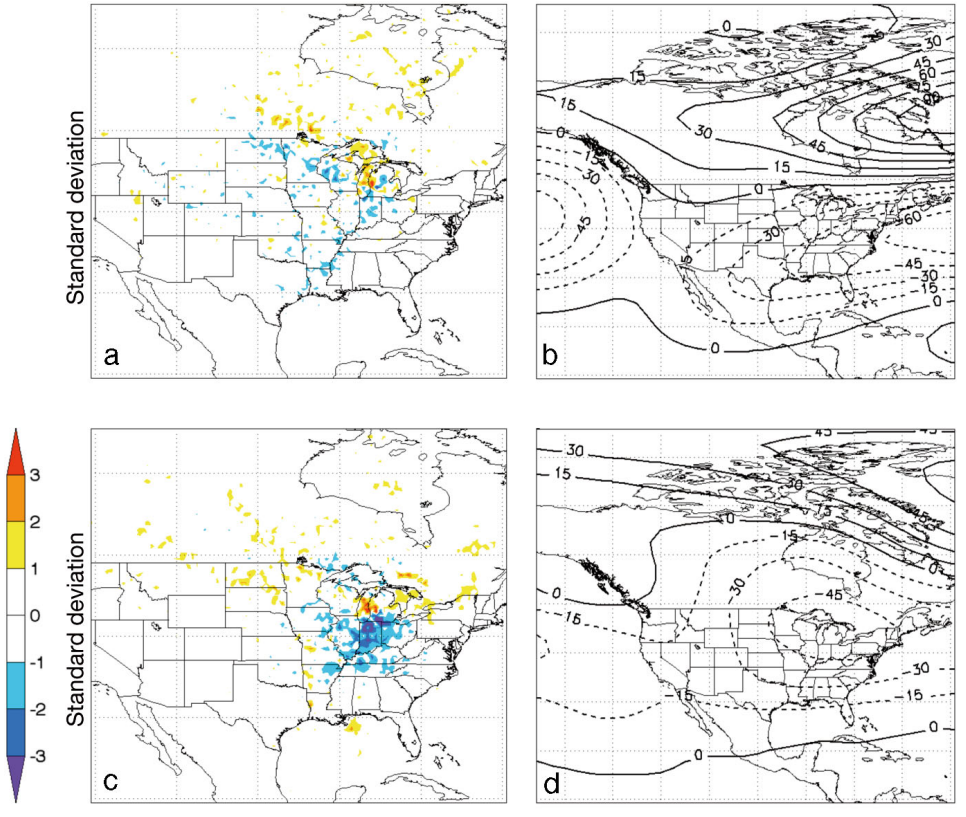

Fig. 8. Seasonal NAO−, NINO+ 925 hPa trajectory anomalies (left) and 500 hPa height (m) anomalies (right): (a,b) winter, (c,d) autumn. See Fig. 3 legend for explanation of colors and lines

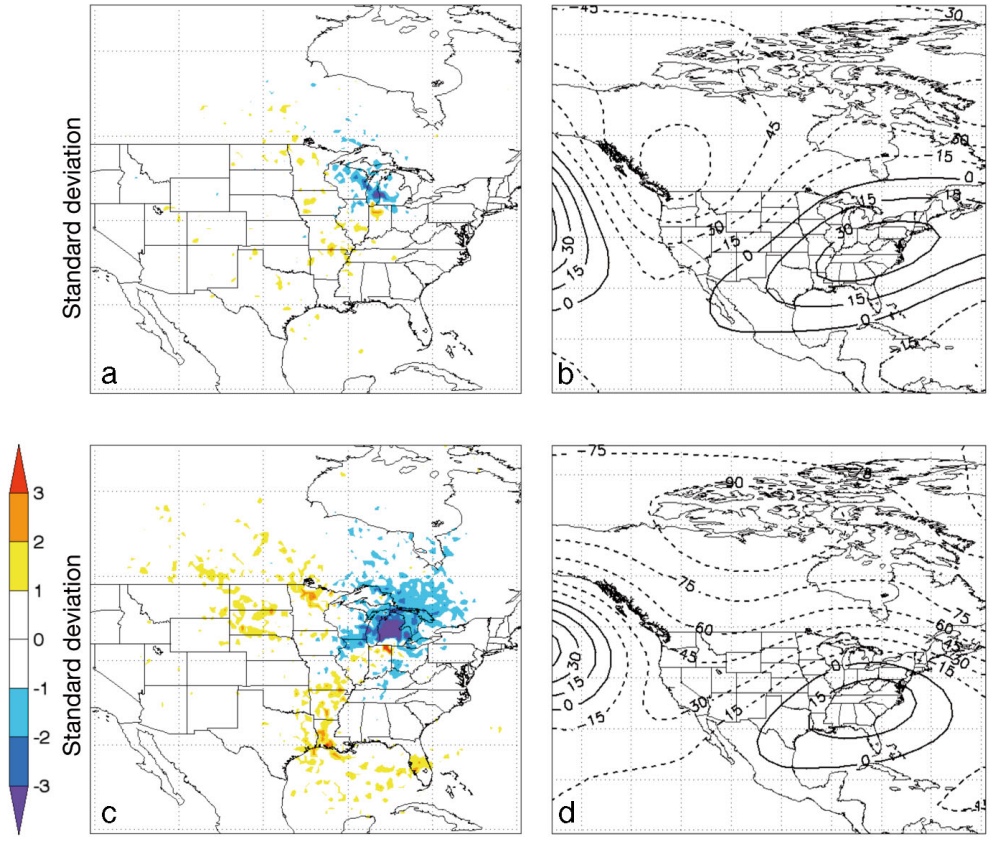

Fig. 9. Seasonal PNA–, NINO– 925 hPa trajectory anomalies (left) and 500 hPa height (m) anomalies (right): (a,b) winter, (c,d) spring. See Fig. 3 legend for explanation of colors and lines

spring (Fig. 3e,f) and summer (Fig. 3g,h). NAO– winters and autumns occurred infrequently (maps not shown), but also presented increased low-level flow from the north, decreased low-level flow from the south, higher-than-normal 500 hPa heights in the region of the Icelandic Low, and below normal height values over the eastern USA. Similar conditions were found when combining NAO– and El Niño (Fig. 8a–d), suggesting that NAO– tends be play the larger role when these 2 strong teleconnections are acting together. Increased northerly flow and decreased 500 hPa heights corresponded to a dry anomaly for winter (–17.2 mm; significant at $\alpha = 0.01$) and a cold anomaly for autumn (–2.0°C; significant at $\alpha = 0.01$). One difference between NAO– alone and NAO– combined with NINO+ is that a stronger pressure gradient emerges during the coexisting pattern. Low-level trajectories originating further from the terminus point also support this, and those 925 hPa trajectories extending far to the north may be responsible for the cold and dry anomalies.

PNA– and NINO– (La Niña) occurred together in winter (10.2% frequency) and in spring (5.4% frequency). Although the trajectory and height patterns for PNA– and La Niña (Fig. 9a–d) are quite similar to those shown for winter PNA– (Fig. 4e,f), when PNA– was combined with La Niña, a stronger pressure gradient emerged, similar to when NINO– was combined with NAO. For both winter and spring, a strong trough is present over western North America and higher-than-normal heights are present over the southeastern USA. For both seasons there is a decrease in northerly low-level flow and an increase in southwesterly low-level flow. During spring for PNA– alone, the flow was somewhat more zonal (Fig. 4h), but when combined with La Niña there is a more distinct trough/ridge pattern. For winter and spring, Michigan was downstream of this trough axis placing it in a suggested area of warm-air advection, although no significant temperature anomaly was present (Table 2). Possible mid-level divergence downstream from the trough, however, may have been responsible for the resulting wet precipitation anomalies for winter (12.9 mm; significant at $\alpha = 0.05$) and spring (13.5 mm; significant at $\alpha = 0.05$).

4. ADDRESSING THE RESEARCH QUESTIONS

(1) Does low-level circulation, as depicted by airflow trajectories, differ from the mean circulation over Michigan during seasons of strong single or coexisting teleconnection patterns?

Few studies have discussed atmospheric teleconnection association with low-level airflow, particularly within the Great Lakes region. Some studies have presented temperature and precipitation associations or have discussed mid-level airflow patterns across the USA (Wallace & Gutzler 1981, Rogers 1984, Leathers et al. 1991, Assel 1992, Rohli & Rogers 1993, Serreze et al. 1998, Changnon et al. 2000, Hu & Feng 2001a, 2001b). However, the present study also considered low-level airflow trajectories for Lower Michigan in an effort to relate atmospheric teleconnections with local-scale climate anomalies of temperature and precipitation. Mid-level circulation shown here typically resembled circulation described in previous teleconnection literature (see Section 1). Associations with temperature and precipitation tended to be most prominent when low-level trajectories had a similar pattern to the overlying mid-level flow. However, in other cases when low-level trajectories differed from mid-level flow, significant temperature and precipitation anomalies were less common. Results presented here indicated that during strong phases of one or more teleconnections, low-level circulation often differs substantially from the respective seasonal airflow climatology, which suggests that teleconnections should be considered in medium- to long-range forecasting for the Great Lakes region.

(2) During months of anomalous circulation associated with teleconnections, can relationships be drawn between the trajectory patterns and local-scale climate?

In most cases the resulting significant temperature and/or precipitation anomalies coincided well with the low-level airflow patterns. For many of the teleconnection combinations, the sign of the temperature and precipitation anomalies shown in Tables 2 & 3 corresponded to earlier teleconnection analyses for the Midwest region, such as cold and dry anomalies during autumn PNA+ conditions. Statistically significant associations provided further support that these relationships may be causal. Tables 2 & 3 highlighted the statistically significant anomalies. By grouping the teleconnection combinations by season, 108 possible seasonal teleconnection combinations were possible. Not all 108 situations occurred. In fact, only 25 combinations were present ≥10 times during a particular season (i.e. a 5.0% seasonal frequency) throughout the 1950–2011 period. Of all seasonal teleconnection combinations studied, 8 combinations were associated with a significant temperature anomaly, and 4 with significant precipitation anomalies. This result is in agreement with previous studies that teleconnection associations with temperature tend to be more common than associations with precipitation (Wallace & Gutzler 1981, Rogers 1984, Leathers et al. 1991, Assel 1992, Serreze et al. 1998).

The results of the present study showed that although relationships between local temperature and precipitation and teleconnection combinations were apparent, significant relationships did not occur in all cases. When considering all frequent seasonal teleconnection combinations, 11 had significant temperature and/or precipitation anomalies, while 14 combinations had neither a significant temperature nor significant precipitation anomaly. As a result, consideration of some seasonal teleconnection combinations may be more important than others in medium- and long-range forecasting. In addition, it is noteworthy that when considering only frequent, coexisting teleconnections, all 5 seasonal combinations described here had a significant temperature or precipitation anomaly (Section 3.4).

(3) Does the association of single or coexisting teleconnections with trajectories and local-scale climate vary by season?

Not all combinations occurred frequently in all seasons. The resulting airflow, temperature, and precipitation anomalies were not always consistent across the seasons of a particular teleconnection combination. Significant temperature and precipitation anomalies occurred in all seasons. One teleconnection combination had a significant temperature anomaly in winter, with 3 in spring, 1 in summer, 3 in autumn. In terms of significant precipitation anomalies, 2 teleconnection combinations had significant anomalies in winter, with 1 in spring, none in summer, and 1 in autumn. Many more neutral teleconnection combinations occurred during spring and summer compared to autumn and winter. During autumn and winter months, the likelihood of having one or more of the NAO, PNA, and NINO3.4 teleconnections in a strong phase was 86%, while during spring and summer months the likelihood was 79%. These results show that the teleconnections were more likely to have strong values during the cooler months than in the warmer months of the year, which is in agreement with previous literature (Wallace & Gutzler 1981, Rogers 1984, 1985, Leathers et al. 1991, Hastenrath & Greishchar 2001).

5. CONCLUDING REMARKS

The study presented here strove to go beyond the work of previous research by considering combinations of coexisting, strong teleconnections within a region that has not gained much attention previously in teleconnection research. Associations between atmospheric teleconnections, 500 hPa height anomalies, and 925 hPa low-level airflow trajectories aided in explaining temperature and precipitation anomalies in Michigan for seasons of single and coexisting teleconnection combinations. This study supports the consideration of teleconnection combinations in future studies in order to more accurately understand observed or modeled climate anomalies. It is my hope that the methods presented here can be used for future climate research, since other teleconnection indices and geographical areas remain open to exploration.

Acknowledgements. The author thanks the anonymous reviewers, and Julie Winkler, Jeffrey Andresen, Joseph Messina (Michigan State University), and David McGinnis (National Science Foundation) for their thoughtful suggestions throughout this research project.

LITERATURE CITED

Aguado E, Burt JE (2012) Understanding weather and climate, 6th edn. Pearson Education, Upper Saddle River, NJ

Angel JR, Isard SA (1998) The frequency and intensity of Great Lakes cyclones. J Clim 11:61–71

Assel RA (1992) Great Lakes winter-weather 700-hPa PNA teleconnections. Mon Weather Rev 120:2156–2163

Assel RA, Rodionov S (1998) Atmospheric teleconnections for annual maximum ice cover on the Laurentian Great Lakes. Int J Climatol 18:425–442

Assel RA, Drobot S, Croley TE (2004) Improving 30-day Great Lakes ice cover outlooks. J Hydrometeorol 5: 713–717

Barnston AG, Livezey RE (1987) Classification, seasonality and persistence of low-frequency atmospheric circulation patterns. Mon Weather Rev 115:1083–1126

Bradbury JA, Dingman SL, Keim BD (2002a) New England drought and relations with large scale atmospheric circulation patterns. J Am Water Resour Assoc 38:1287–1299

Bradbury JA, Keim BD, Wake CP (2002b) U.S. East Coast trough indices at 500 hPa and New England winter climate variability. J Clim 15:3509–3517

Budikova D (2005) Impact of the Pacific Decadal Oscillation on relationships between temperature and the Arctic Oscillation in the USA in winter. Clim Res 29:199–208

Budikova D (2008) Effect of the Arctic Oscillation on precipitation in the eastern USA during ENSO winters. Clim Res 37:3–16

Changnon SA, Hilberg SD, Kunkel KE (2000) El Niño 1997-1998 in the Midwest. Contract Report No. 2000-10, Midwestern Regional Climate Center, Champaign, IL

Coleman JS, Rogers JC (2003) Ohio River Valley winter moisture conditions associated with the Pacific-North American teleconnection pattern. J Clim 16:969–981

D'Aleo JS, Grube PG (2002) The Oryx resource guide to El Niño and La Niña. Oryx Press, Westport, CT

Eichler T, Higgins W (2006) Climatology and ENSO-related variability of North American extratropical cyclone activity. J Clim 19:2076–2092

Englehart PJ, Douglas AV (2003) Assessing warm season drought episodes in the central United States. J Clim 16: 1831–1842

Gershunov A, Barnett TP (1998) ENSO influence on intraseasonal extreme rainfall and temperature frequencies in the contiguous United States: observations and model results. J Clim 11:1575–1586

Hardy JW, Henderson KG (2003) Cold front variability in the southern United States and the influence of atmospheric teleconnection patterns. Physical Geography 24:120–137

Harrison DE, Larkin NK (2002) Cold events: anti-El Niño? In Glantz MH (ed) La Niña and its impacts: facts and speculation. United Nations University Press, Tokyo, p 237–241

Hastenrath S, Greishchar L (2001) The North Atlantic Oscillation in the NCEP-NCAR reanalysis. J Clim 14: 2404–2413

Henderson KG, Robinson PJ (1994) Relationships between the Pacific/North American teleconnection patterns and precipitation events in the south-eastern USA. Int J Climatol 14:307–323

Higgins RW, Leetmaa A, Kousky VE (2002) Relationships between climate variability and winter temperature extremes in the United States. J Clim 15:1555–1572

Hu Q, Feng S (2001a) Variations of teleconnection of ENSO and interannual variation in summer rainfall in the central United States. J Clim 14:2469–2480

Hu Q, Feng S (2001b) Climatic role of the southerly flow from the Gulf of Mexico in interannual variations in summer rainfall in the central United States. J Clim 14: 3156–3171

Huang J, Higuchi K, Shabbar A (1998) The relationship between the North Atlantic Oscillation and El Niño-Southern Oscillation. Geophys Res Lett 25:2707–2710

Kalnay E, Kanamitsu M, Kistler R, Collins W and others (1996) The NCEP/NCAR 40-year reanalysis project. Bull Am Meteorol Soc 77:437–471

Kistler R, Kalnay E, Collins W, Saha S and others (2001) The NCEP-NCAR 50-year reanalysis: monthly means CD-ROM and documentation. Bull Am Meteorol Soc 82: 247–267

Konrad CE (1998) Intramonthly indices of the Pacific/North American teleconnection pattern and temperature regimes over the United States. Theor Appl Climatol 60: 11–19

Leathers DJ, Yarnal B, Palecki MA (1991) The Pacific/North American teleconnection pattern and United States climate. Part I: Regional temperature and precipitation associations. J Clim 4:517–528

Mote TL (1996) Influence of ENSO on maximum, minimum, and mean temperatures in the southeast United States. Phys Geogr 17:497–512

Renwick JA, Wallace JM (1996) Relationships between North Pacific wintertime blocking, El Niño, and the PNA pattern. Mon Weather Rev 124:2071–2076

Rodionov SN (1994) Association between winter precipitation and water level fluctuations in the Great Lakes and

atmospheric circulation patterns. J Clim 7:1693–1706
Rodionov S, Assel R (2000) Atmospheric teleconnection patterns and severity of winters in the Laurentian Great Lakes basin. Atmos-Ocean 38:601–635
Rodionov S, Assel RA (2003) Winter severity in the Great Lakes region: a tale of two oscillations. Clim Res 24: 19–31
Rodionov S, Assel R, Herche L (2001) Tree-structured modeling of the relationship between Great Lakes ice cover and atmospheric circulation patterns. J Gt Lakes Res 27: 486–502
Rogers JC (1984) The association between the North Atlantic Oscillation and the Southern Oscillation in the Northern Hemisphere. Mon Weather Rev 112:1999–2015
Rogers JC (1985) Atmospheric circulation changes associated with the warming over the northern North Atlantic in the 1920s. J Clim Appl Meteorol 24:1303–1310
Rogers JC, Coleman JS (2004) Ohio winter precipitation and stream flow associations to Pacific atmospheric and oceanic teleconnection patterns. Ohio J Sci 104:51–59
Rogers JC, Rohli RV (1991) Florida citrus freezes and polar anticyclones in the Great Plains. J Clim 4:1103–1113
Rohli RV, Rogers JC (1993) Atmospheric teleconnections and citrus freezes in the southern United States. Phys Geogr 14:1–15
Ropelewski CF, Halpert MS (1986) North American precipitation and temperature patterns associated with the El Niño/Southern Oscillation (ENSO). Mon Weather Rev 114:2352–2362
Ropelewski CF, Halpert MS (1987) Global and regional scale precipitation patterns associated with the El Niño/Southern Oscillation. Mon Weather Rev 115:1606–1626
Ropelewski CF, Halpert MS (1989) Precipitation patterns associated with the high index phase of the Southern Oscillation. J Clim 2:268–284
Serreze MC, Clark MP, McGinnis DL, Robinson DA (1998) Characteristics of snowfall over the eastern half of the United States and relationships with principal modes of low-frequency atmospheric variability. J Clim 11:234–250
Shadbolt RP, Waller EA, Messina JP, Winkler JA (2006) Source regions of lower-tropospheric airflow trajectories for the lower peninsula of Michigan: a 40-year air mass climatology. J Geophys Res 111:D21117. doi:10.1029/2005JD006657
Sheridan SC (2003) North American weather-type frequency and teleconnection indices. Int J Climatol 23:27–45
Thompson DWJ, Wallace JM (2001) Regional climate impacts of the Northern Hemisphere annular mode. Science 293:85–89
Vega AJ, Rohli RV, Henderson KG (1998) The Gulf of Mexico mid-tropospheric response to El Niño and La Niña forcing. Clim Res 10:115–125
Wallace JM, Gutzler DS (1981) Teleconnections in the geopotential height field during the Northern Hemisphere winter. Mon Weather Rev 109:784–812
Wanner H, Brönnimann S, Casty C, Gyalistras D and others (2001) North Atlantic Oscillation—concepts and studies. Surv Geophys 22:321–382
Yarnal B, Leathers DJ (1988) Relationships between interdecadal and interannual climatic variations and their effect on Pennsylvania climate. Ann Assoc Am Geogr 78:624–641
Yin ZY (1994) Moisture condition in the south-eastern USA and teleconnection patterns. Int J Climatol 14:947–967

Editorial responsibility: Oliver Frauenfeld, College Station, Texas, USA

Submitted: January 9, 2012; Accepted: July 17, 2012
Proofs received from author(s): November 6, 2012